Impact of Photonic Bandgap Hollow-Core Fiber Loss Wavelength Dependence on the Performance of RFOG

Maxime Descampeaux, Benoit Debord, Foued Amrani, Gilles Feugnet, Fetah Benabid, Fabien Bretenaker, Frédéric Gérôme

Impact of Photonic Bandgap Hollow-Core Fiber Loss Wavelength Dependence on the Performance of RFOG

Maxime Descampeaux
Thales
Avionics
Châtellerault, France
maxime.descampeaux
@fr.thalesgroup.com

Gilles Feugnet
Thales
Research & Technology
Palaiseau, France
gilles.feugnet@thalesgroup.com

Fabien Bretenaker
LuMIN
CNRS, Université Paris-Saclay
Gif-sur-Yvette, France
fabien.bretenaker
@universite-paris-saclay.fr

Benoit Debord
GPPMM group, XLIM
CNRS, Université de Limoges
Limoges, France
benoit.debord@xlim.fr

Fetah Benabid
GPPMM group, XLIM
CNRS, Université de Limoges
Limoges, France
f.benabid@xlim.fr

Frédéric Gérôme
GPPMM group, XLIM
CNRS, Université de Limoges
Limoges, France
frederic.gerome@xlim.fr

Foued Amrani
GPPMM group, XLIM
CNRS, Université de Limoges
Limoges, France
foued.amrani@xlim.fr

***Abstract*— A resonant fiber ring cavity based on a photonic-bandgap hollow-core fiber is described and characterized. We explore the fine spectral dependence of the transmission losses of this cavity and their impact on the performances of the resulting resonator fiber optic gyroscope (RFOG).**

Keywords—Resonant gyroscope, Hollow-core fiber, loss wavelength dependence, fiber ring cavity, transmission spectrum

I. INTRODUCTION

The passive resonator fiber optic gyroscope (RFOG) makes use of the Sagnac effect to measure the angular velocity by comparing the resonance frequencies of two counter-propagating modes of a passive resonator [1]. The resonance frequencies of the two counter propagating beams are tracked by locking the probe optical frequencies at resonance. Thanks to the light recirculation inside the cavity, the RFOG has the potentiality to achieve the same performances as the interferometric fiber optic gyroscope (IFOG) with a smaller fiber length.

The sensitivity of an RFOG based on conventional single mode silica-core fibers can be limited by different sources of noise and bias such as the nonlinear Kerr effect and polarization fluctuations, which are indistinguishable from the Sagnac effect. The non-linear Kerr effect corresponds to a dependence of the refractive index on the intensity of light propagating in the silica core of the fiber. Consequently, a small intensity difference between the two counter-propagating waves gives rise to a nonreciprocal index difference resulting in a bias in the gyroscope response [2].

To overcome those limitations inherent to RFOGs based on silica-core fibers, considerable efforts have been produced to develop gyroscopes based on hollow-core fiber [3,4]. The structure of those fibers consists in periodic photonic crystals surrounding an air core located at its center. The light mode thus mainly propagates in the air core, reducing the bias induced by the nonreciprocal Kerr effect in the RFOG. In addition, the hollow-core fiber contributes to reduce the gyro temperature sensitivity compared to standard single mode fibers [5].

Whatever the type of fiber used in the RFOG, one of the main source of noise is the backscattering-induced noise caused by the interferences between the propagating light and the backreflected light (Rayleigh scattering) [6]. This source of noise can be eliminated by probing the cavity resonances on different modes separated by one or more free spectral ranges (FSR) of the cavity [7].

In a previous work, our research team developed a hollow-core Kagome fiber ring resonator with a finesse of 23 and reached a bias stability of 0.45°/h over 0.5s [8]. This fiber had a core diameter of approximately 60µm and was coiled on a diameter of 60cm. In order to reduce the dimension of the device prototype, we developed a packaged 8cm-diameter fiber ring cavity based on a photonic-bandgap hollow-core fiber (PBG-HCF), less sensitive to bending losses, with a core diameter of approximately 15µm, shown in Figure 1. Contrary to the Kagome fiber, this PBG-HCF can be coiled with smaller diameter and is supposed be less sensitive to the mechanical vibration. This fiber prototype was tailored for our gyroscope.

In Section II, we present the packaging of the resonator based on this PBG-HCF and explain the link between the fiber transmission losses and the cavity transmission losses. Section III aims at reporting the frequency-dependence of the

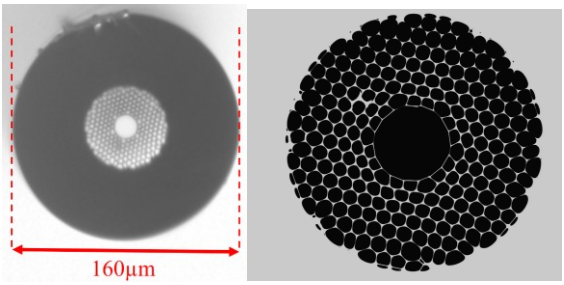

Fig. 1: Optical images of the PBG-HCF cross-section

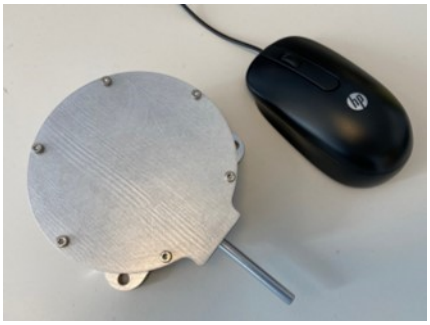

Fig. 2: Picture of the packaging of the 8cm-diamterer PBG-HCF ring resonator (computer mouse for scale)

transmission losses of the fiber ring cavity. We then analyze how this phenomenon affects the error-signal used to lock the laser frequency to the cavity resonance and the gyroscope performances when adjacent modes are probed to avoid backscattering.

II. Fiber Ring Cavity

The structure of the packaging of the cavity is shown in Figure 2. In particular, the arrangement is designed to couple the light in and out of the cavity based on hollow-core fiber from the standard polarization maintaining fiber. Since no fibered coupler based on hollow core fiber is commercially available, it is necessary to have a free-space portion in the resonator to couple the light into the two types of fibers and to close the cavity itself. The beam alignment relies on a special design assuring that only one polarization state can resonate.

Once the cavity is packaged, one can monitor the light transmitted or reflected by this cavity. In order to evaluate the dependence of the cavity transmission versus the transmission of the fiber, one needs a simple theoretical model. To this aim, we consider a fiber ring cavity closed by two mirrors. We neglect the distance corresponding to free space propagation between the two fiber ends (few centimeters) and take a cavity length $L = 22$ m. The free spectral range (FSR) of the cavity is noted $\Delta\nu_{\mathrm{FSR}} = 13.8$ MHz. We note T the intensity transmission inside the cavity that takes into account the fiber propagation losses and the input and output coupling efficiencies of the cavity mode to the fiber. By taking into account the amplitude transmission and reflection coefficients of the two mirrors ($t_{1,2}$ and $r_{1,2}$), we obtain the amplitude transmission of the cavity probed in transmission $F(\nu)$ as a function of the laser input frequency noted ν.

$$F(\nu) = \frac{t_1 t_2 \sqrt{T} e^{i2\pi\nu/\Delta\nu_{\mathrm{FSR}}}}{1 - r_1 r_2 \sqrt{T} e^{i2\pi\nu/\Delta\nu_{\mathrm{FSR}}}} \quad (1)$$

Equation (1) is similar to the well-known formula of [9]. If we note I_0 the light intensity incident on the cavity, the intensity transmitted by the cavity $I(\nu)$ is

$$I(\nu) = I_0 |F(\nu)|^2. \quad (2)$$

If ν_{res} is one resonance frequency of the cavity, the cavity intensity transmission $I(\nu_{\mathrm{res}})/I_0$ is equal to $|F(\nu_{\mathrm{res}})|^2$.

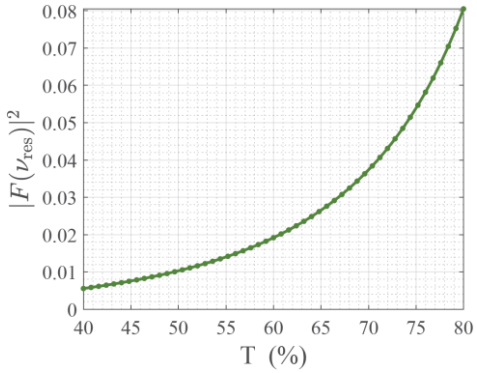

Fig. 3: Intensity transfer function of the cavity probed in transmission at resonance frequency $\boldsymbol{\nu_{\mathrm{res}}}$ versus $\boldsymbol{T}$ the intracavity transmission

Figure 3 shows the evolution of $|F(\nu_{\mathrm{res}})|^2$ as a function of T, the intracavity mirror-to-mirror transmission coefficient through the PBG-HCF. As expected, intensity transmitted by the cavity at resonance decreases with inscreasing intracavity losses. This plot can be used to evaluate the degradation of the fiber transmission by monitoring the cavity intensity transmission degradation, as it will be described in the following section.

III. Experiments and Analysis

A. Measurement of the cavity transmission loss

The packaged 8cm-diameter fiber ring cavity described in Section II is temperature stabilized. Its transmission is probed in the CW direction with a laser initially tuned at $\lambda = 1550.078$ nm. We apply a triangular voltage to the laser frequency modulation input. The transmitted beam is measured with a photodiode. Figure 4(a) and 4(b) show the transmission spectrum for a laser frequency sweep of about 3 cavity free spectral ranges (FSR). As can be seen in the zoom of Figure 4(b), the maximum transmitted intensity is not exactly the same for the three observed resonances, while the incident intensity is measured to be identical. This evidences the presence of intra-cavity optical losses that depend on small variations of the laser frequency. We used equations (1) and (2) to fit the transmission spectrum and found a finesse of 14 and $T = 70\%$. Then, the phase of the incident light is modulated at frequency $f_{mod} = 500$ kHz and the photodiode signal is demodulated at f_{mod} to generate an error signal shown in Figure 4(c). One can see in Figure 4(d) that there is a linear relation between the error signal slope around resonance and the intensity transmitted resonance [10]. This confirms that the presence of intra-cavity optical losses is directly affecting the amplitude of the error signal and its slope around resonance.

The frequency-dependence of these losses is further highlighted in Figure 5 that shows the evolution of the maximum photodiode signal at resonance (peak signal) when the laser central wavelength is scanned over a range of 0.1 nm. This corresponds to the spectrum of the cavity transmission loss. Those irregular variations can reach up to 75% within a wavelength range of 20 pm around 1550.11 nm. As, the maximum transmission of the PBG-HCF was measured to be of the order of 80%, the maximum cavity transmission is theoretically $|F(\nu_{\mathrm{res}})|^2 = 0.08$ as shown in Figure 3. Consequently, a peak signal variation of 75% on the cavity

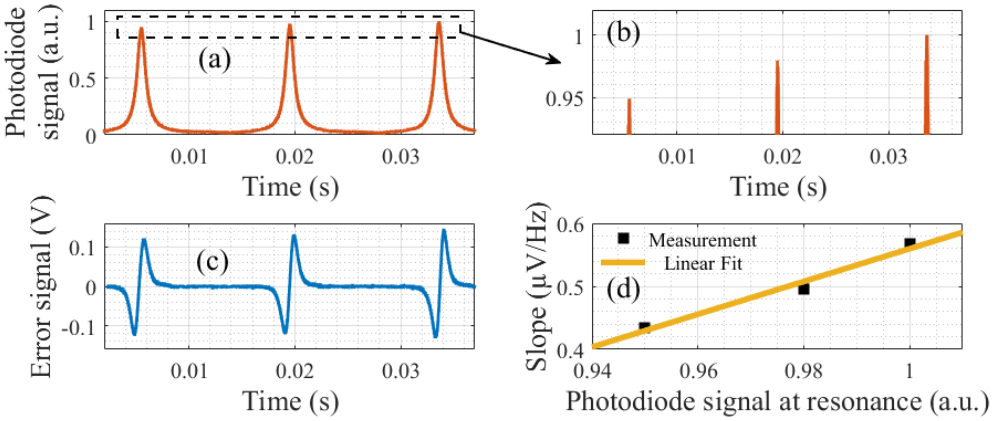

Fig. 4: Measured (a,b) photodiode signal monitoring the cavity transmission and (c) error signal when scanning the laser frequency at 10 Hz around the central wavelength 1550.078 nm. (d) Measured error signal slope versus photodiode signal at resonance and its linear fit.

transmission corresponds to $|F(\nu_{\mathrm{res}})|^2 = 0.02$, meaning that the fiber transmission has decreased down to 60%.

This phenomenon might be a consequence of the polarization fluctuation inside the cavity and of the presence of surface modes [11]. These modes are primarily localized in the silica core-surround of the fiber and can couple to the core mode under the right phase-matching conditions. Here, these modes are weakly coupling and usually unresolved with ordinary optical spectral analyzer. This kind of frequency-dependent losses in HCF has already been observed and can be explained by the enhancement of the coupling to surface modes due to a tight coil [12]. The next subsection aims a discussing about how those transmission losses compromise the angular velocity measurement.

B. Analysis of the impact on the gyroscope performances

As explained in the introduction, the RFOG measures the angular velocity by comparing the recorded resonance frequencies of two counter propagating beams. In the setup of [8], two acousto-optic modulators (AOM) are used to shift the counter propagating frequencies by ± 110 MHz to probe the cavity on two different modes and avoid backscattering. The AOM frequencies are adjusted to track the cavity resonances that are modified by the Sagnac effect when the gyro rotates. In this case, the two modes are separated by approximately $\Delta\nu = 220$ MHz, which corresponds to roughly $\Delta\lambda = 2$ pm. In Figure 5, we see that two signals at resonance separated by around $\Delta\lambda = 2$ pm are very different. Consequently, the two servo-loops will have two different and unstable error signal slopes and compromise the measurement.

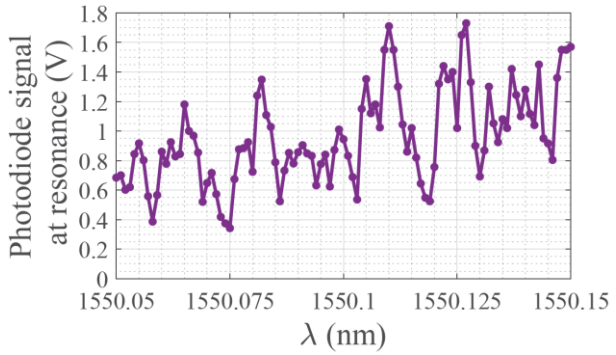

Fig. 5: Measured evolution of the maximum photodiode signal at resonance versus the laser central wavelength $\boldsymbol{\lambda}$.

Even if we probe the cavity with the same mode, the laser frequency dependence of the losses will affect the measurements, as the very strong condition on the equality of the ±1 sidebands amplitude for correct locking will not be completed. One can develop the same calculation of the error signal as [13] to explore the consequence of an imbalance between the two sidebands amplitude. Equation (3) shows the electric field E_{out} transmitted by the cavity with a difference of power 2α between the two sideband amplitudes. J_k is the k[th] order Bessel function, $\beta = 1.08$ rad is the modulation depth, $E_0 = \sqrt{I_0}$ is the incident electric field and $\omega_{mod} = 2\pi f_{mod}$ the modulation frequency.

$$E_{\mathrm{out}} = E_0 \begin{pmatrix} J_0(\beta)F(\omega)e^{i\omega t} \\ +(1+\alpha)J_1(\beta)F(\omega+\omega_{mod})e^{i(\omega+\omega_{mod})t} \\ -(1-\alpha)J_1(\beta)F(\omega-\omega_{mod})e^{i(\omega-\omega_{mod})t} \end{pmatrix} \quad (3)$$

$$V_{err} = 2\mathrm{G}I_0J_1(\beta)J_0(\beta)\left[f_{mod}\frac{d|F(\nu)|^2}{d\nu} + 2\alpha|F(\nu)|^2\right] \quad (4)$$

Equation (4) is the expression of the error signal V_{err} obtained when calculating $|E_{\mathrm{out}}|^2$ and demodulating it at f_{mod}. G is the optoelectronic gain (in V/W) that contains the response of the detector. Assuming $\alpha = 0$ leads to the original expression in [13].

In transmission, the incident beams are modulated at f_{mod} equals to half the cavity linewidth $\Gamma = \Delta\nu_{\mathrm{FSR}}/\mathrm{Finesse} \approx 1$ MHz. From fitting the experimental data in Figure 4(c), we found $2\mathrm{G}I_0J_1(\beta)J_0(\beta) = 4.8$ V while $|F(\nu_{\mathrm{res}})|^2 = 0.038$ for $T = 70$ % from Figure 3. In the example of Figure 4(b), the transmitted intensity variation is 5% over a frequency range of 2 times the FSR, so the intensity difference over the range frequency separating the two sidebands can be extrapolate and approximated to 0.2 %. This is equivalent to $\alpha = 0.001$ in Eq. (4) and leads to a voltage bias of 370 µV at resonance frequency ν_{res}. This voltage bias corresponds to a frequency bias of 740 Hz for an error signal slope of 0.5 µV/Hz. As our 8cm-diameter ring resonator has a scale factor of 900 Hz/(°/s), this corresponds to a bias in the order of 1 °/s in the angular velocity measurement. The problem is that this bias is unstable as the laser central frequency and the cavity resonance frequency drift.

This is of course the worst case where all the difference is on one sideband. A more optimistic case would be the central laser frequency being at a minimum of these frequency-dependent losses. However, we did observe that these frequencies, at which the losses are minimum, vary day to day so this is not a convenient situation for a high accuracy instrument such as a gyroscope of inertial measurement.

IV. Conclusion

To conclude, we presented the packaging of our resonator based on a PBG-HCF. We report the high-resolution spectral dependence of the transmission loss of the cavity and their impact on our RFOG. We suspect the coupling to surface mode of the PBG-HCF to be the main contributor of those discrepancies. The cavity transmission losses are frequency dependant and we estimate that the fiber transmission can vary from 80% to 60% within a wavelength range of 20 pm. We explain how this phenomenon might limit of the performances of a resonant PBG-HCF optical gyroscope. Thus, a hollow-core fiber model free of surface modes must be identified. Conversely, the RFOG high resolution can be used as a metrology tool of the hollow-core fibers modal properties to improve their design.

Acknowledgment

We thank Kylia for designing and assembling the cavity. We also thank Frédéric Delahaye and Alexandre Gorse from GLOphotonics company for their contribution in fiber fabrication campaign.

Funding from Région Nouvelle Aquitaine and ANR.

References

[1] R. E. Meyer, S. Ezekiel, D. W. Stowe, and V. J. Tekippe, “Passive fiber-optic ring resonator for rotation sensing,” Opt. Lett. 8(12), 644–646 (1983).

[2] Gilles Feugnet, Alexia Ravaille, Sylvain Schwartz, Fabien Bretenaker, “Analysis of the design of a passive resonant miniature optical gyroscope based on integrated optics technologies,” Opt. Eng. 56(10), 107109 (2017), doi: 10.1117/1.OE.56.10.107109.

[3] Glen A. Sanders, Austin A. Taranta, Chellappan Narayanan, Eric Numkam Fokoua, Seyedmohammad Abokhamis Mousavi, Lee K. Strandjord, Marc Smiciklas, Thomas D. Bradley, John Hayes, Gregory T. Jasion, Tiequn Qiu, Wes Williams, Francesco Poletti, and David N. Payne, "Hollow-core resonator fiber optic gyroscope using nodeless anti-resonant fiber," Opt. Lett. 46, 46-49 (2021)

[4] Xinxin Suo, Haicheng Yu, Jing Li, and Xudong Wu, "Transmissive resonant fiber-optic gyroscope employing Kagome hollow-core photonic crystal fiber resonator," Opt. Lett. 45, 2227-2230 (2020)

[5] Mutugala, U.S., Numkam Fokoua, E.R., Chen, Y. et al. Hollow-core fibres for temperature-insensitive fibre optics and its demonstration in an Optoelectronic oscillator. Sci Rep 8, 18015 (2018). https://doi.org/10.1038/s41598-018-36064-1

[6] A. Ravaille et al., "In-Situ Measurement of Backscattering in Hollow-Core Fiber Based Resonant Cavities," in IEEE Photonics Journal, vol. 9, no. 4, pp. 1-7, Aug. 2017, Art no. 7104507, doi: 10.1109/JPHOT.2017.2713441.

[7] H. Ma, J. Zhang, L. Wang and Z. Jin, "Development and Evaluation of Optical Passive Resonant Gyroscopes," in Journal of Lightwave Technology, vol. 35, no. 16, pp. 3546-3554, 15 Aug.15, 2017, doi: 10.1109/JLT.2016.2587667.

[8] Alexia Ravaille, Gilles Feugnet, Benoît Debord, Frédéric Gérôme, Fetah Benabid, and Fabien Bretenaker, "Rotation measurements using a resonant fiber optic gyroscope based on Kagome fiber," Appl. Opt. 58, 2198-2204 (2019)

[9] Fabre, Claude & Grynberg, Gilbert & Aspect, Alain. (2010). Introduction to Quantum Optics: From the Semi-classical Approach to Quantized Light, p.232. 10.1017/CBO9780511778261.

[10] Shihao Yin, Wenyao Liu, Enbo Xing, Ziwen Pan, Yu Tao, Jiangbo Zhu, Jun Tang, Jun Liu, “Suppression of laser intensity fluctuation in resonator optical gyro by a simple light intensity feedback technique,” Opt. Eng. 59(3), 036112 (2020), doi: 10.1117/1.OE.59.3.036112

[11] James A. West, Charlene M. Smith, Nicholas F. Borrelli, Douglas C. Allan, and Karl W. Koch, "Surface modes in air-core photonic band-gap fibers," Opt. Express 12, 1485-1496 (2004)

[12] Therice A. Morris and Michel J. F. Digonnet, "Broadened-Laser-Driven Polarization-Maintaining Hollow-Core Fiber Optic Gyroscope," J. Lightwave Technol. 38, 905-911 (2020)

[13] Eric D. Black , "An introduction to Pound–Drever–Hall laser frequency stabilization", American Journal of Physics 69, 79-87 (2001) https://doi.org/10.1119/1.128666